RESEARCH ARTICLE

Cell Culture and Tissue Engineering



Check for updates

The impact of temozolomide and lonafarnib on the stemness marker expression of glioblastoma cells in multicellular spheroids

Pinaki S. Nakod¹ | Raghu Vamsi Kondapaneni¹ | Brandon Edney² | Yonghyun Kim¹ | Shreyas S. Rao¹ |

Correspondence

Shreyas S. Rao, Department of Chemical and Biological Engineering, The University of Alabama, Tuscaloosa, AL 35487, USA. Email: srao3@eng.ua.edu

Funding information

National Science Foundation, Grant/Award Number: 1604677; Alabama EPSCoR Graduate Research Fellowship

Abstract

Glioblastoma multiforme (GBM) is a highly malignant brain tumor with a poor prognosis. The GBM microenvironment is highly heterogeneous and is composed of many cell types including astrocytes and endothelial cells (ECs) along with tumor cells, which are responsible for heightened resistance to standard chemotherapeutic drugs such as Temozolomide (TMZ). Here, we investigated how drug treatments impact stemness marker expression of GBM cells in multicellular tumor spheroid (MCTS) models. Co- and tri-culture MCTS constructed using U87-MG GBM cells, astrocytes, and/or ECs were cultured for 7 days. At Day 7, 5 μM lonafarnib (LNF), 100 μM TMZ, or combination of 5 μ M LNF + 100 μ M TMZ was added and the MCTS were cultured for an additional 48 h. We assessed the spheroid sizes and expression of stemness markers- NESTIN, SOX2, CD133, NANOG, and OCT4- through qRT-PCR and immunostaining. Following 48 h treatment with LNF, TMZ or their combination (LNF + TMZ), the spheroid sizes decreased compared to the untreated control. We also observed that the expression of most of the stemness markers significantly increased in the LNF + TMZ treated condition as compared to the untreated condition. These results indicate that drug treatment can influence the stemness marker expression of GBM cells in MCTS models and these aspects must be considered while evaluating therapies. In future, by incorporating other relevant cell types, we can further our understanding of their crosstalk, eventually leading to the development of new therapeutic strategies.

KEYWORDS

coculture, glioblastoma, spheroids, stemness, triculture

1 | INTRODUCTION

Glioblastoma multiforme (GBM), a grade IV brain tumor, is extremely malignant and lethal with a median survival period of only 12–14 months.¹ The current therapy involving neurosurgical resection followed by radiation and chemotherapy regimens has not significantly increased the poor prognosis of GBM.² The standard

chemotherapeutic drug- temozolomide (TMZ) improves patient survival by only 2.5 months when combined with radiotherapy; whereas multiple new targeted therapies have failed to improve patient outcomes.^{3,4} This can be, in part, attributed to the lack of understanding of the GBM tumor microenvironment, which is responsible for the heightened resistance to chemo- and radio-therapy, thereby rendering the treatment ineffective.^{2,3,5} Thus, studying GBM tumors in vitro



¹Department of Chemical and Biological Engineering, The University of Alabama, Tuscaloosa, Alabama, USA

²Department of Biological Sciences, The University of Alabama, Tuscaloosa, Alabama, USA

utilizing biomimetic culture systems that capture key aspects of the microenvironment might eventually help devise therapeutic approaches to improve disease outcomes.⁶

The GBM microenvironment is composed of not only tumor cells but also diverse cell types such as astrocytes and endothelial cells (ECs). These cells support GBM stem cell-like cells and/or induce dedifferentiation of tumor cells to a tumor-initiating (stem cell-like) phenotype and contribute to their heightened resistance to therapeutic treatments.^{5,7-10} For example, astrocytes have been shown to increase GBM survival and resistance against TMZ in coculture condition as compared to monoculture condition. 11-14 ECs are an important component of the perivascular niche and are responsible for increased resistance of GBM cells against TMZ. 15-17 GBM stem cell-like cells are a subpopulation of GBM cells that express stemness-related markers like NESTIN, SOX2, CD133, NANOG, and OCT4, have been reported to have high self-renewal, multilineage differentiation, and heightened resistance to therapeutic treatments.^{8,9} These cells can also trans-differentiate into ECs and enhance the resistance to antiangiogenic therapy, thereby resulting in treatment failure in GBM.^{3,18}

Most of the studies have utilized two-dimensional tissue culture polystyrene (TCPS) as culture substrates to investigate the effects of chemotherapeutic drugs on GBM-astrocytes or GBM-EC cocultures. 2,13,19 While these studies have provided key insights into the role of cellular cues in determining tumor cell response to therapy, they lack the complexity of the microenvironment found in 3D structures. Multicellular tumor spheroids (MCTS) are 3D structures that more accurately reflect the complex tumor microenvironment features such as cell organization in layers with different proliferation rates, presence of cell-cell interactions and signaling, and formation of nutrient and oxygen gradients. 20 However, only few studies have employed 3D MCTS models to coculture GBM cells with astrocytes/ECs, and only one has utilized GBM cells with astrocytes and ECs in a 3D triculture MCTS model. 6,11,12,21,22 Moreover, to the best of our knowledge, the effect of drug treatment on the stemness marker expression of GBM cells in a 3D co- or tri-culture MCTS model has not been reported.

Temozolomide (TMZ), a DNA alkylating agent, has been used as a standard chemotherapeutic drug for GBM. It achieves its cytotoxic effect mainly by methylating the O⁶ position of guanine.²³ However, TMZ treatment also results in drug resistance owing to the heterogeneity of glioma cells, upregulation of O⁶-methylguanine DNA methyltransferase (MGMT), DNA repair, and signal transducer and activator of transcription 3 (STAT3).^{23,24} Lonafarnib (LNF) is a potent farnesyltransferase inhibitor (FTI) with less myelosuppressive side effects that is in clinical trials against GBM.²⁵ LNF has the potential to inhibit the farnesylation of a variety of proteins such as RhoB, RAS, prelamin A, prelamin B, and CCAX phosphatase, which are involved in cell proliferation and maintenance.²⁶ Previous work by Chaponis et al., has shown that combining cytostatic agent LNF with cytotoxic agent TMZ, increased the activity of TMZ and radiation in vitro as well as in vivo.²⁵ Building on this finding, we sought to investigate how these treatments impact GBM stemness marker expression in 3D co- and tri-culture MCTS models.²⁵

Here, we utilized a 1:4 GBM-astrocytes co-culture model, 1:9 GBM-EC co-culture model, and 1:4:9 GBM-astrocytes-EC triculture

model based on our previous findings.⁶ Specifically, at these culture ratios, we observed an enhanced expression of stemness markers-NESTIN, SOX2, CD133, NANOG, and OCT4 at the gene and protein level, when GBM cells were cultured in the presence of astrocytes and/or ECs as compared to when cultured individually.⁶ In this study, we have utilized these 3D co- and tri-culture MCTS to study the impact of LNF, TMZ, and their combination (LNF + TMZ) on the growth profile and expression of stemness markers, particularly, *NES*, *SOX2*, *CD133*, *NANOG*, and *OCT4*.

2 | MATERIALS AND METHODS

2.1 | Cell culture

Human U87-MG GBM cells were cultured in Eagle's Minimum Essential Medium (EMEM, ATCC) supplemented with 10% fetal bovine serum (FBS) and 1% penicillin-streptomycin (VWR Life Science). Mouse astrocytes (C8D1A; ATCC) and human umbilical vein endothelial cells (HUVECs, Lonza) were cultured as previously described.⁶ All cells were maintained in a humidified 5% CO₂ environment at 37°C and were harvested upon reaching 70%–80% confluency using Trypsin (Gibco).

2.2 | Construction of 3D co- and tri-culture MCTS

3D MCTS were constructed according to the liquid overlay technique using a 96-well round-bottom ultra-low attachment spheroid microplate (Corning[®]) as previously described.⁶ Briefly, all cell suspensions were prepared in their respective media - U87-MG in EMEM complete medium, astrocytes in DMEM complete medium, and HUVECs in EGM-2 complete medium. GBM-astrocytes and GBM-EC coculture MCTS were prepared by adding 100 µl of respective cell suspensions such that the resulting composition of cells was 1:4 GBM:astrocytes and 1:9 GBM:EC where the number of U87-MG cells were fixed at 5000 cells/well. The coculture MCTS were maintained in 1:1 EMEM: DMEM for GBM-astrocytes or 1:1 EMEM:EGM-2 media composition for GBM-ECs. For the triculture MCTS, 67 μl of each cell suspension was transferred into a well such that the resulting composition of 1:4:9 GBM:astrocytes:EC was achieved where the number of U87-MG cells were fixed at 5000 cells/well. The triculture MCTS were maintained in 1:1:1 EMEM:DMEM:EGM-2 media composition. After cell seeding, plates were centrifuged at 1000×g for 10 min and incubated at 37°C in a humidified 5% CO2 environment. All co- and tri-culture MCTS were cultured up to Day 7 and half the medium was replenished every 2 days.

2.3 | Drug treatment

Lonafarnib (LNF; Sigma Aldrich) and Temozolomide (TMZ; Sigma Aldrich) were reconstituted in DMSO according to the manufacturer's

3 of 12

protocol and were diluted in culture media for treatment. At Day 7, GBM:astrocytes, GBM:EC, and triculture MCTS were treated with 5 μ M LNF, 100 μ M TMZ or their combination (5 μ M LNF + 100 μ M TMZ) for 48 h. These concentrations were chosen based on previous studies that have demonstrated that TMZ (100 µM) targeted MGMT and telomerase activity, and LNF (5 µM) inhibited the neurosphere formation in GBM cells. 25,27-34

2.4 Optical microscopy and image analysis

3D MCTS were monitored using an Olympus IX83 microscope with a spinning disc confocal attachment. The size and the cross-sectional area of the spheroids were analyzed using ImageJ software (NIH) as described previously.⁶ Area and perimeter of the spheroids were obtained using ImageJ to get Circularity = 4π Area/(Perimeter²).

2.5 Cell viability within MCTS

Cell viability within the co- and tri-culture MCTS was monitored using the Live/Dead Cell Assay kit (Thermo Fisher Scientific) using the manufacturer's protocol. Briefly, 48 h after drug treatment, 8 µM Calcein AM dilution and 8 μM Ethidium homodimer dilution was prepared in the corresponding media depending on the culture condition. Later, drug media was replaced with 100 µl of Calcein AM (for staining viable cells) and 100 ul of Ethidium homodimer (for staining dead cells) and incubated for 90 min at 37°C. Next, spheroids were washed with PBS before imaging.

Quantitative real-time polymerase chain reaction (qRT-PCR)

gRT-PCR was performed on RNA samples obtained from co- and triculture MCTS as described previously.⁶ Briefly, to assess the marker expression at 48 h time point after drug treatment, 3-5 spheroids per replicate were harvested using p200 pipette with tip cut halfway to facilitate easy removal of spheroids while preserving their integrity and pooled. RNA was extracted and transcribed into cDNA for quantification. Gene expression was quantified by qRT-PCR (StepOnePlus Real-Time PCR System, Applied Biosystems) using PowerUp SYBR Green Master Mix (Applied Biosystems) and the appropriate gene-specific primers (Table S1). Relative expression of the genes compared to the housekeeping gene (GAPDH) were calculated using $\Delta\Delta C_t$ method, where $\Delta C_t = \Delta C_{t,gene of interest} - \Delta C_{t,GAPDH}$. Coculture and triculture data was normalized to the respective untreated control MCTS.

2.7 Immunofluorescence staining

Co- and tri-culture MCTS were dissociated into single cells and immunofluorescence staining was performed as previously described.⁶ To identify the different cell types in co- and tri-culture MCTS, U87-MG cells were labeled with CellTracker™ Green CMFDA dye while constructing the spheroids. Briefly, the dissociated single cells were fixed with 4% paraformaldehyde, permeabilized using 0.25% Triton-X and blocked with 5% bovine serum albumin (BSA). The cells were incubated with primary antibodies (Table S2) overnight at 4°C following which cells were incubated with Alexa Fluor 594-conjugated goat anti-rabbit secondary antibody (A-11012, Invitrogen) at 4°C for 1 h, and counterstained with DAPI nuclear stain for 5 min. Cells with a positive green, red, and blue signal were identified as tumor cells positive for the corresponding marker and the percentage positive tumor cells for the corresponding marker was evaluated through manual counting using multi-point tool in ImageJ software (NIH) as previously described.⁶

2.8 Statistical analysis

The data is presented as mean ± standard error. Statistical analysis was performed with JMP® software and the significance was calculated using Student's t-test or analysis of variance followed by Tukey's HSD post-hoc analysis. All the experiments were repeated independently at least twice. With all analyses, the significance level was set at $p \le 0.05$.

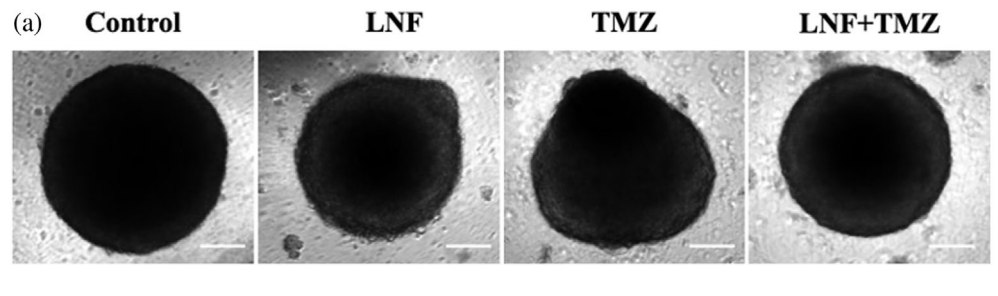
RESULTS

3.1 Coculture MCTS after drug treatment for 48 h

GBM-astrocytes and GBM-EC coculture MCTS were cultured according to the liquid overlay technique. We constructed coculture MCTS with tumor cells at a fixed initial seeding density of 5000 cells/well and only increasing the initial seeding density of astrocytes to 20,000 cells/well and ECs to 45,000 cells/well resulting in coculture ratios of 1:4 and 1:9, respectively.⁶ At these coculture ratios, we observed an enhanced expression of stemness markers- NESTIN, SOX2, CD133, NANOG, and OCT4 at the gene and protein levels, when GBM cells were cultured in the presence of astrocytes or ECs as compared to when cultured individually.6

GBM-astrocytes coculture MCTS 3.1.1

Majority of the tumor cells and astrocytes self-assembled to form a loosely aggregated spheroid at Day 1 and the spheroid became more compact over a period of 7 days similar to our previous observation.⁶ Following 48 h treatment with LNF, the spheroid size decreased significantly $(p \le 0.05)$ by 1.1-fold as compared to the untreated control (Figure 1). Similarly, following 48 h treatment with combination of LNF + TMZ, the spheroid size decreased significantly ($p \le 0.05$) by 1.1-fold as compared to the untreated control. Similar sizes of spheroids were observed when GBM-astrocyte coculture MCTS were treated



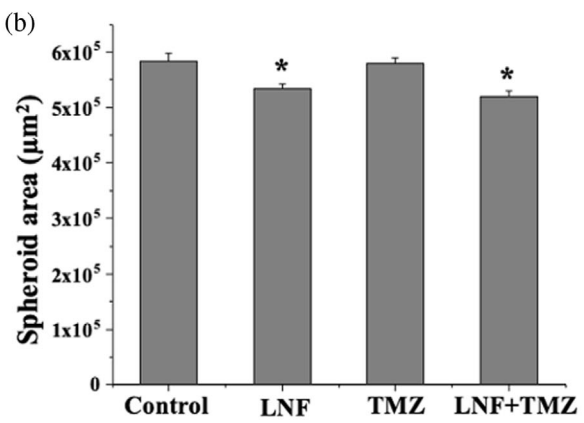


FIGURE 1 Characterization of 3D GBM-Astrocyte coculture MCTS 48 h after drug addition. (a) Representative images of GBM cells cocultured with astrocytes at a ratio of 1:4. Scale bar = $200 \mu m$. (b) Quantification of spheroid areas 48 h after drug addition. Values represent mean \pm standard error. N \geq 15 replicates per condition. * $p \leq 0.05$ compared to control and TMZ conditions

with LNF or LNF + TMZ. After 48 h treatment with TMZ, no significant change (p > 0.05) in the spheroid size was observed as compared to the untreated control. Circularity measurements obtained from spheroids indicated mostly circular morphology for all conditions. The circularity decreased with LNF and TMZ treatment compared to untreated controls, however, no changes were noted in LNF + TMZ treated spheroids versus untreated controls (Figure S1a). Cell viability staining qualitatively indicated more dead cells in LNF and LNF + TMZ treated spheroids compared to untreated control and TMZ treated spheroids (Figure S2).

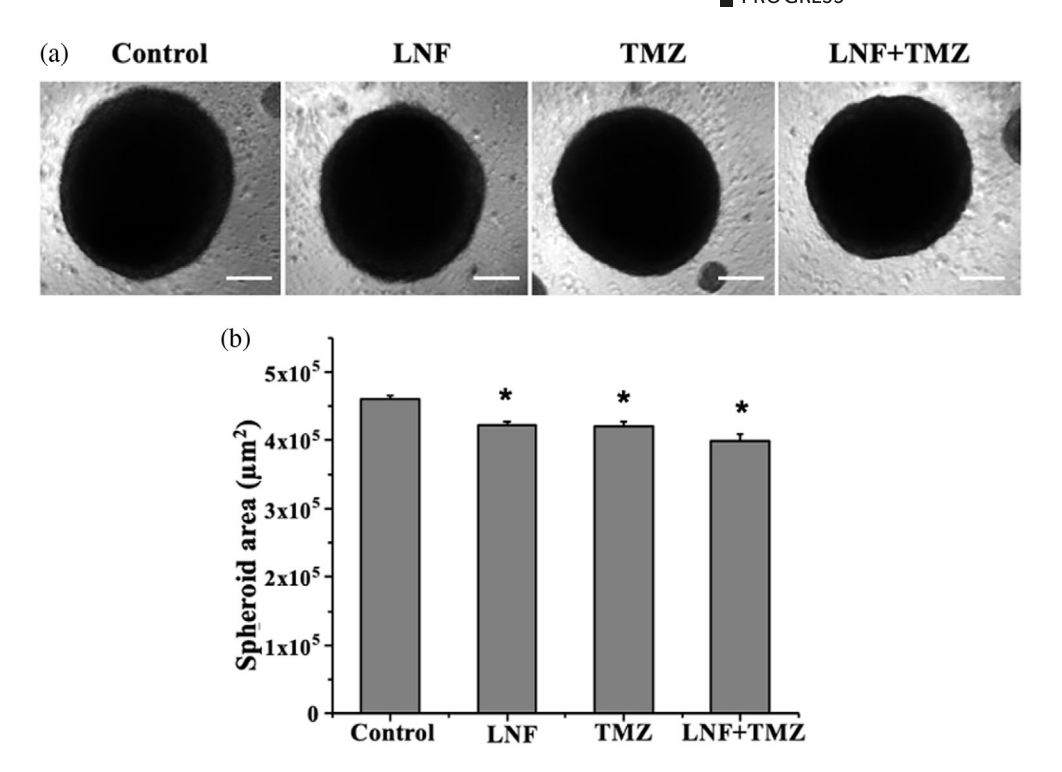
3.1.2 | GBM-EC coculture MCTS

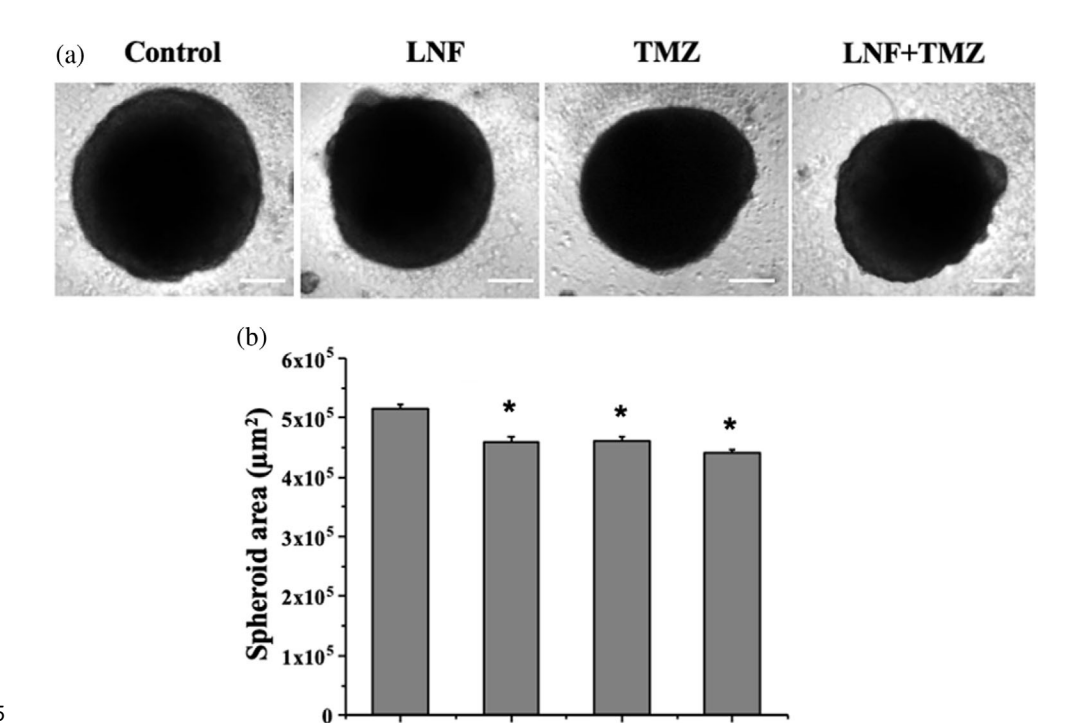
Similar to GBM-astrocytes coculture MCTS, majority of the tumor cells and EC self-assembled to form a loosely aggregated spheroid at Day 1 and the GBM-EC coculture MCTS became more compact over a period of 7 days. Following 48 h treatment with LNF, the spheroid size decreased significantly ($p \le 0.05$) by 1.1-fold as compared to the untreated control (Figure 2). Similarly, following 48 h treatment with TMZ, the spheroid size decreased significantly ($p \le 0.05$) by 1.1-fold as compared to the untreated control. Similar sizes of spheroids were observed when GBM-EC coculture MCTS were treated with only LNF or TMZ. After 48 h treatment with LNF + TMZ, the spheroid size decreased significantly ($p \le 0.05$) by 1.15-fold as compared to the untreated control. Circularity measurements obtained from spheroids indicated mostly circular morphology for all conditions where circularity was similar for the untreated and drug treated spheroids (Figure S1b). Cell viability staining qualitatively indicated more dead cells in LNF, TMZ and LNF + TMZ treated spheroids compared to untreated control spheroids (Figure S3).

3.2 | GBM-astrocytes-EC triculture MCTS after drug treatment for 48 h

For the triculture model, tumor cells were cultured with astrocytes and ECs in the ratio of 1:4:9 where the initial number of tumor cells was fixed at 5000 cells/well. We have utilized a 1:4:9 GBM-astrocytes-EC triculture model based on our previous results in which we observed an enhanced expression of stemness markers- NESTIN, SOX2, CD133, NANOG, and OCT4 at the gene and protein levels, when GBM cells were cultured in the presence of astrocytes and ECs as compared to when cultured individually. Majority of the tumor cells, astrocytes, and EC selfassembled to form a loosely aggregated spheroid at Day 1 and the triculture MCTS became more compact over a period of 7 days similar to our previous observation.⁶ Following 48 h treatment with LNF, the spheroid size decreased significantly $(p \le 0.05)$ by 1.1-fold as compared to the untreated control (Figure 3). Similarly, following 48 h treatment with TMZ, the spheroid size decreased significantly ($p \le 0.05$) by 1.1-fold as compared to the untreated control. Similar sizes of spheroids were observed when the triculture MCTS were treated with only LNF or TMZ. After 48 h treatment with LNF + TMZ, the spheroid size decreased significantly ($p \le 0.05$) by 1.2-fold as compared to the untreated control. Circularity measurements obtained from spheroids indicated mostly circular morphology for all conditions, where untreated control spheroids had significantly higher circularity than all the drug treated spheroids (Figure S1c). Cell viability staining qualitatively indicated more dead cells in LNF, TMZ and LNF + TMZ treated spheroids compared to untreated control spheroids (Figure S4).

FIGURE 2 Characterization of 3D GBM-EC coculture MCTS 48 h after drug addition. (a) Representative images of GBM cells cocultured with endothelial cells at a ratio of 1:9. Scale bar = $200 \mu m$. (b) Quantification of spheroid areas 48 h after drug addition. Values represent mean \pm standard error. N ≥ 15 replicates per condition. * $p \le 0.05$ compared to control





LNF

Control

FIGURE 3 Characterization of 3D triculture MCTS 48 h after drug addition. (a) Representative images of GBM cells cocultured with astrocytes and endothelial cells at a ratio of 1:4:9. Scale bar = 200 μm. (b) Quantification of spheroid areas 48 h after drug addition. Values represent mean \pm standard error. *N* ≥ 15 replicates per condition. **p* ≤ 0.05 compared to control

3.3 | Stemness marker expression of coculture MCTS after drug treatment for 48 h

We investigated the impact of drug treatment on the expression of NES, SOX2, CD133, NANOG, and OCT4 as these markers have been commonly used for the identification of stemness phenotype in GBM cells. $^{35-37}$

3.3.1 | GBM-astrocytes coculture MCTS

TMZ

After 48 h treatment with LNF + TMZ, the expression of *NES* increased significantly ($p \le 0.05$) by 1.5-, 2.3-, and 1.6-fold as compared to untreated control, LNF, and TMZ treated conditions, respectively (Figure 4a). The expression of *NES* was unaltered in LNF and TMZ treated conditions as compared to control (p > 0.05). The

LNF+TMZ

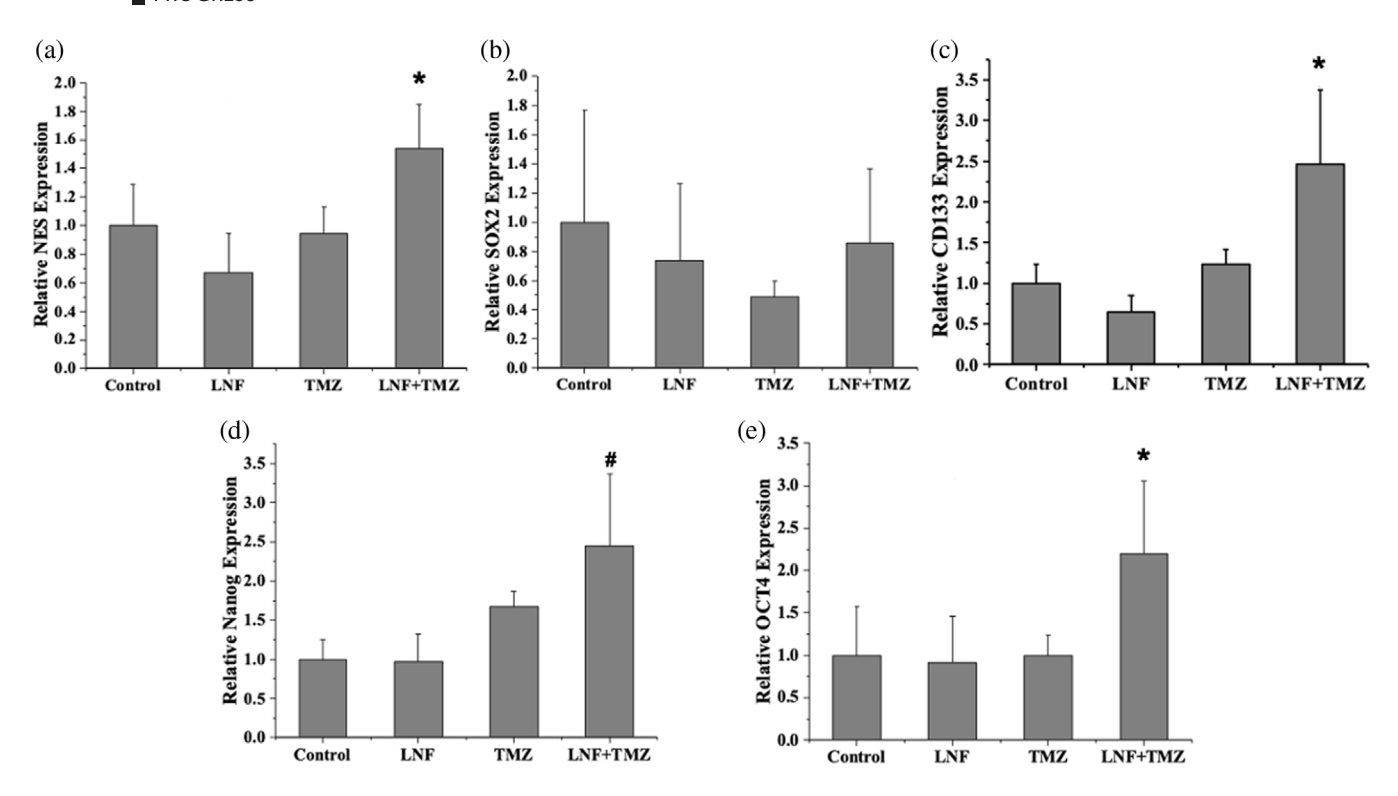


FIGURE 4 Expression of stemness markers in a 3D GBM-astrocyte coculture MCTS model post-treatment with LNF, TMZ or their combination. Relative expression of (a) *NES*, (b) *SOX2*, (c) *CD133*, (d) *NANOG*, and (e) *OCT4*. Relative expression normalized to the respective untreated control condition. Values represent mean \pm standard error. N = 3 biological replicates per condition which were independently setup. * $p \le 0.05$ compared to the respective control and LNF conditions.

expression of SOX2 remained unaltered after treatment with LNF, TMZ, or LNF + TMZ (Figure 4b). The expression of CD133 increased significantly ($p \le 0.05$) in LNF + TMZ treated condition by 2.5-, 3.8-. and 2-fold as compared to untreated control, LNF, and TMZ treated conditions, respectively (Figure 4c). The expression of CD133 was unaltered in LNF and TMZ treated conditions as compared to control (p > 0.05). The expression of NANOG increased significantly (p \leq 0.05) in LNF + TMZ treated condition by 2.4- and 2.5-fold as compared to untreated control and LNF treated conditions, respectively (Figure 4d). The expression of NANOG increased by 1.7-fold in TMZ treated condition as compared to the untreated control, however this was not statistically significant (p > 0.05). The expression of OCT4 increased significantly ($p \le 0.05$) in LNF + TMZ treated condition by 2.2-, 2.4-, and 2.2-fold as compared to untreated control, LNF, and TMZ treated conditions, respectively (Figure 4e). The expression of OCT4 was unaltered in LNF and TMZ treated conditions as compared to control (p > 0.05). We then evaluated the expression of these markers at the protein level for all GBM-astrocyte coculture MCTS conditions through immunofluorescence staining. We observed a significant increase ($p \le 0.05$) in the percentages of NESTIN-positive and SOX2-positive tumor cells in LNF + TMZ treated condition as compared to LNF treated condition (Figures S5 and S6). Percentage of NESTIN-positive tumor cells decreased significantly ($p \le 0.05$) in LNF treated condition as compared to the untreated control. The percentage of CD133-positive tumor cells increased significantly ($p \le 0.05$) in LNF + TMZ treated condition as compared to untreated control, LNF

and TMZ treated conditions (Figure S7). The percentage of NANOG-positive tumor cells was not impacted after treatment with LNF and/or TMZ (Figure S8). The percentage of OCT4-positive tumor cells increased significantly ($p \le 0.05$) in LNF + TMZ treated condition as compared to untreated control, LNF and TMZ treated conditions (Figure S9).

3.3.2 | GBM-EC coculture MCTS

The expression of NES remained unaltered after 48 h treatment with LNF, TMZ, or LNF + TMZ (Figure 5a). The expression of NES increased by 1.3-fold in TMZ treated condition as compared to the untreated condition, however, this was not statistically significant (p > 0.05). Similarly, the expression of SOX2 remained unaltered after 48 h treatment with LNF, TMZ, or LNF + TMZ (Figure 5b). The expression of SOX2 increased by 2.2-fold in TMZ treated condition as compared to the untreated condition, however, this was not statistically significant (p > 0.05). The expression of CD133 increased significantly ($p \le 0.05$) in LNF + TMZ treated condition by 2.6-, 2.2-, and 2.3-fold as compared to untreated control, LNF, and TMZ treated conditions, respectively (Figure 5c). The expression of CD133 was unaltered in LNF and TMZ treated conditions as compared to control (p > 0.05). The expression of NANOG increased significantly $(p \le 0.05)$ in LNF + TMZ treated condition by 2- and 1.9-fold as compared to untreated control and LNF treated conditions,

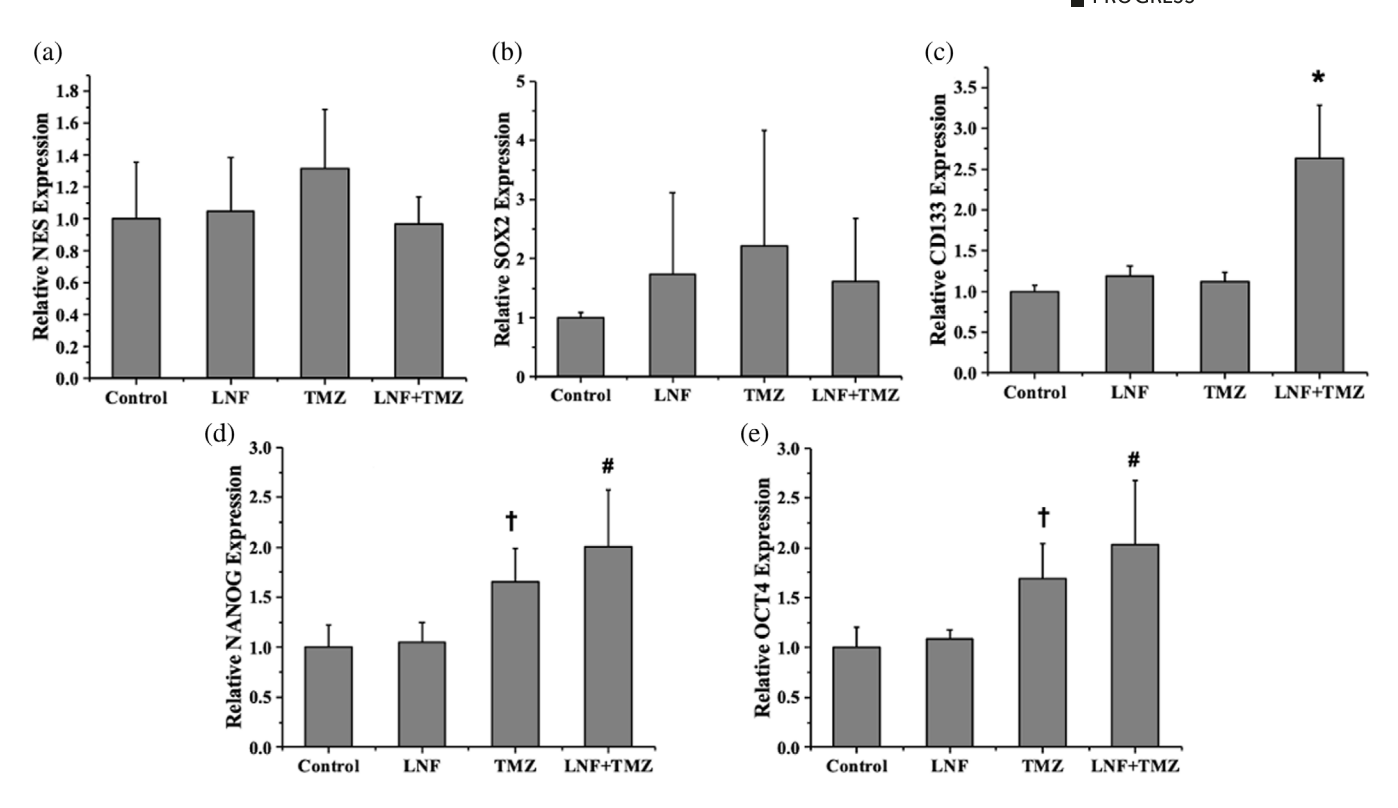


FIGURE 5 Expression of stemness markers in a 3D GBM-EC coculture MCTS model post-treatment with LNF, TMZ or their combination. Relative expression of (a) *NES*, (b) *SOX2*, (c) *CD133*, (d) *NANOG*, and (e) *OCT4*. Relative expression normalized to the respective untreated control condition. Values represent mean \pm standard error. N=3 biological replicates per condition which were independently setup. * $p \le 0.05$ compared to the respective control, LNF, and TMZ conditions. * $p \le 0.05$ compared to the respective control condition

respectively (Figure 5d). The expression of NANOG increased significantly ($p \le 0.05$) in TMZ treated condition by 1.6-fold as compared to untreated control. The expression of OCT4 increased significantly $(p \le 0.05)$ in LNF + TMZ treated condition by 2- and 1.9-fold as compared to untreated control and LNF treated conditions, respectively (Figure 5e). The expression of OCT4 increased significantly $(p \le 0.05)$ in TMZ treated condition by 1.7-fold as compared to untreated control. We then evaluated the expression these markers at the protein level for all GBM-EC coculture MCTS conditions through immunofluorescence staining. Similar percentages of NESTIN-positive and SOX2-positive tumor cells were observed for the treated or untreated conditions (Figures S10 and S11). We observed a significant increase ($p \le 0.05$) in the percentage of CD133-positive tumor cells in LNF + TMZ treated condition as compared to untreated control condition (Figure S12). Percentage of NANOG-positive tumor cells increased significantly in TMZ treated condition compared to LNF treated condition (Figure S13). We observed a significant increase ($p \le 0.05$) in the percentage of NANOG-positive tumor cells in LNF + TMZ treated condition as compared to untreated control and LNF treated conditions. Similarly, we observed a significant increase ($p \le 0.05$) in the percentage of OCT4-positive tumor cells in LNF + TMZ treated condition as compared to untreated control and LNF treated conditions (Figure S14).

3.4 | Stemness marker expression of triculture MCTS after drug treatment for 48 h

After 48 h treatment with LNF + TMZ, the expression of NES increased significantly ($p \le 0.05$) by 1.9-, 1.9-, and 1.6-fold as compared to untreated control, LNF, and TMZ treated conditions, respectively (Figure 6a). The expression of NES was unaltered in LNF and TMZ treated conditions as compared to control (p > 0.05). The expression of SOX2 increased significantly ($p \le 0.05$) in TMZ treated condition by twofold and 1.6-fold as compared to untreated control and LNF treated conditions, respectively (Figure 6b). The expression of SOX2 increased significantly ($p \le 0.05$) in LNF + TMZ treated condition by 1.6-fold as compared to untreated control. The expression of CD133 increased significantly ($p \le 0.05$) in LNF + TMZ treated condition by 2.5-, 2.1-, and 1.8-fold as compared to untreated control, LNF, and TMZ treated conditions, respectively (Figure 6c). The expression of CD133 was unaltered in LNF and TMZ treated conditions as compared to control (p > 0.05). The expression of NANOG increased significantly ($p \le 0.05$) in LNF + TMZ treated condition by 2.5- and 2.1-fold as compared to untreated control and LNF treated conditions, respectively (Figure 6d). The expression of NANOG increased significantly ($p \le 0.05$) in TMZ treated condition by 2.2- and 1.9-fold as compared to untreated control and LNF treated conditions, respectively. The expression of OCT4 increased significantly

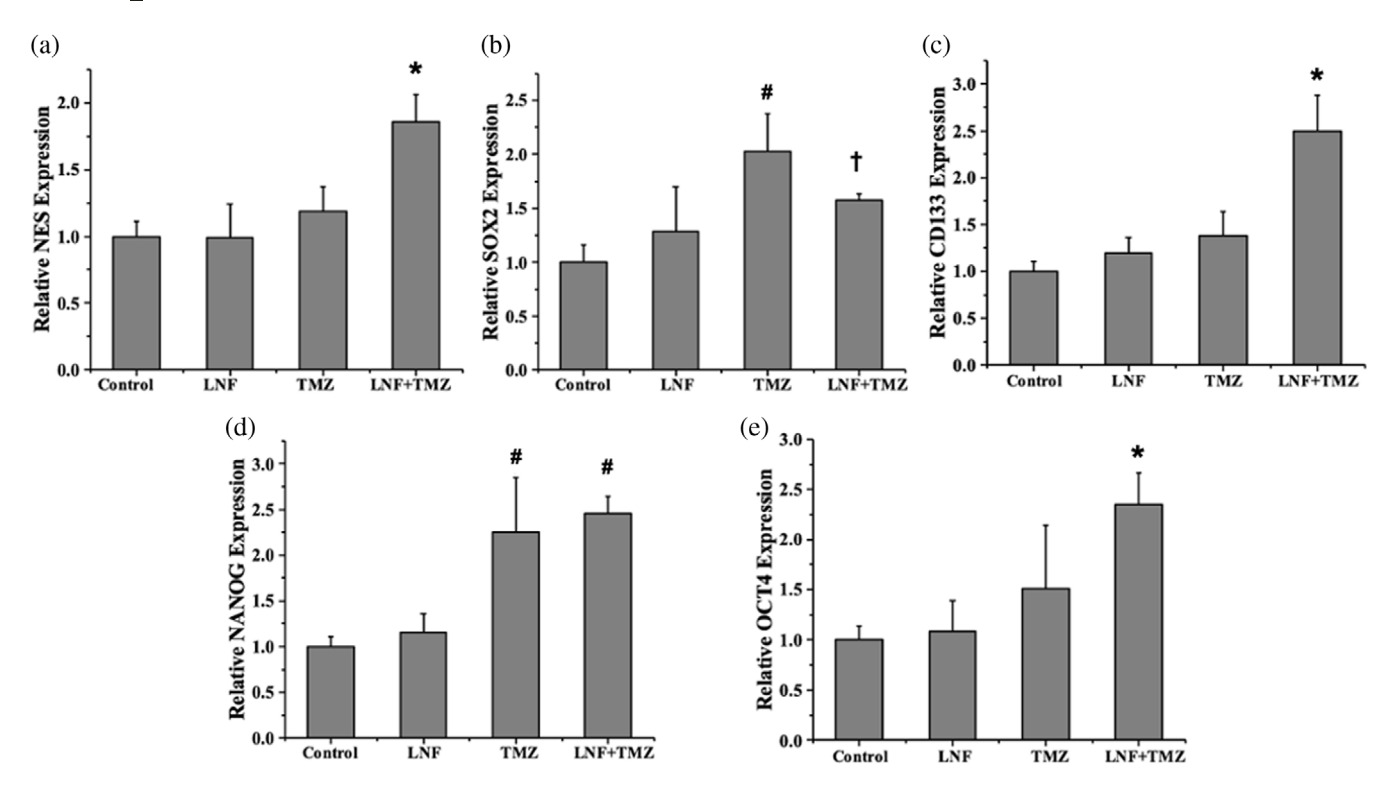


FIGURE 6 Expression of stemness markers in a 3D triculture MCTS model post-treatment with LNF, TMZ or their combination. Relative expression of (a) NES, (b) SOX2, (c) CD133, (d) NANOG, and (e) OCT4. Relative expression normalized to the respective untreated control condition. Values represent mean \pm standard error. N=3 biological replicates per condition which were independently setup. * $p \le 0.05$ compared to the respective control, LNF, and TMZ conditions. * $p \le 0.05$ compared to the respective control condition

(p ≤ 0.05) in LNF + TMZ treated condition by 2.3-, 2.1-, and 1.6-fold as compared to untreated control, LNF, and TMZ treated conditions, respectively (Figure 6e). The expression of *OCT4* was unaltered in LNF and TMZ treated conditions as compared to control (p > 0.05). We then evaluated the expression these markers at the protein level for all triculture MCTS conditions through immunofluorescence staining. Similar percentage of NESTIN-positive tumor cells were observed for the treated or untreated conditions (Figure S15). We observed a significant increase in the percentages of SOX2-positive, CD133-positive, and NANOG-positive tumor cells in TMZ and LNF + TMZ treated conditions as compared to the untreated control and LNF treated conditions (Figures S16, S17, and S18). Similar percentage of OCT4-positive tumor cells were observed for the treated or untreated conditions (Figure S19).

4 | DISCUSSION

In this study, we have utilized 3D co- and tri-culture MCTS composed of GBM tumor cells with astrocytes and/or ECs to study the impact of therapeutics such as TMZ and/or LNF on the stemness marker expression of GBM cells. So far, very few studies have employed MCTS models comprising of GBM cells with astrocytes or ECs to investigate the impact of chemotherapeutic drugs. 11,12,22 Also, to the best of our knowledge, the impact of chemotherapeutic drugs on the

stemness marker expression of GBM cells has not been previously evaluated in a relevant 3D co- or tri-culture MCTS model. Our current study bridges this gap by demonstrating the impact of LNF, TMZ, or their combination on the stemness marker expression of GBM cells in 3D co- and tri-culture MCTS for the first time.

The tumor microenvironment provides biophysical, biochemical, and cellular cues to the tumor cells, and has a crucial role in their maintenance as well as response to therapy. Chemotherapeutic testing in vitro has typically been performed using only GBM tumor cells in model systems that typically involve tumor cells cultured as adherent monolayers or liquid suspension on 2D TCPS. However, these conventional models do not reflect the multicellular microenvironment comprised of native cells such as astrocytes and ECs, which are typically associated with GBM and are responsible for the survival and heightened chemotherapeutic resistance of tumor cells. Here, we have utilized a 3D MCTS model that provides essential cell-cell and cell-extracellular matrix interactions. Such interactions are crucial in dictating in the tumor cell phenotype. 38,39

For our study, we have utilized a well-established GBM cell line-U87-MG cultured in the presence of serum. When grown adherently, U87 cells typically have lower expression of stemness markers; compared to cells grown in serum-free conditions, which exhibit higher expression of stemness markers.⁴⁰ In addition, other studies have found an increased expression of stemness markers (NESTIN, SOX2, CD133, NANOG, OCT 3/4, and CD44) in serum grown U87 cells

when cultured as MCTS compared to when cultured as an adherent monolayer. 41-43 Here, we have utilized 1:4 GBM-astrocytes coculture model, 1:9 GBM-EC co-culture model, and 1:4:9 GBM-astrocytes-EC triculture model as we had previously observed an enhanced expression of stemness markers- NESTIN, SOX2, CD133, NANOG, and OCT4 in these models.⁶ Increased efficacy of LNF and TMZ combination treatment against GBM cells (monoculture) in conventional 2D in vitro models as well as in vivo has been observed previously.²⁵ Specifically, Chaponis and colleagues demonstrated that the combination of LNF and TMZ inhibited neurosphere formation in GBM cells, however, the impact of LNF and/or TMZ on the expression of stemness markers was not evaluated.²⁵ Here, we observed that the treatment with LNF, TMZ, or their combination significantly decreased the spheroid sizes of GBM-astrocytes, GBM-EC, and triculture MCTS as compared to the untreated control showing that the MCTS were sensitive to the treatments. Such a decrease in spheroid size has been observed in GBM monoculture and GBM-astrocytes coculture spheroids after treatment with TMZ. 11,12,44-46 Also, we observed that coand tri-culture spheroids assumed a more irregular shape after treatment with LNF, TMZ, or their combination as compared to the untreated control spheroids. This might be attributed to the disaggregation of outer layers of spheroids in response to the drugs, which has been observed previously with MCTS models.46-50

We previously demonstrated that the stemness marker expression of GBM cells increased when cultured with astrocytes and/or ECs in 3D MCTS models.⁶ Here, we have observed that the expression of stemness markers- NESTIN, SOX2, CD133, NANOG, and OCT4- significantly increased in response to LNF + TMZ treatment in GBM-astrocytes, GBM-EC as well as triculture MCTS. In addition, the expression of some of the stemness markers significantly increased in response to TMZ treatment in GBM-EC (NANOG and OCT4) and triculture MCTS (SOX2 and NANOG). Other studies have also found an increased stemness marker expression of GBM cells in response to TMZ in conventional 2D TCPS models as well as in vivo. 24,51-53 This has been attributed to the de-differentiation of tumor cells to stemcell like phenotype, enrichment of stem-cell like population, and increase in the expression of stemness markers-SOX2, CD133, OCT4in presence of hypoxia-inducible factors that are stabilized during chemotherapeutic stress.51 TMZ has also been found to increase the expression of stemness markers (SOX2 and CD133) in GBM-EC 2D in vitro models as well as in vivo.⁵² No changes in the expression of stemness markers in LNF-treated MCTS could be attributed to FTI selectively targeting GBM cells over stem-like tumor cells.⁵⁴ Further investigation is needed to identify the compensatory mechanisms that might be upregulated in the tumor cells to overcome the effects of LNF, TMZ, or their combinatory treatment. We also confirmed the expression of stemness markers at the protein level through immunostaining and these results were largely consistent with qRT-PCR for most of the markers except for NESTIN and NANOG in the case of GBM-astrocytes MCTS, and NESTIN and OCT4 in the case of triculture MCTS for LNF + TMZ treated conditions. For glioma cells, such discrepancies in the mRNA level and protein expression of stemness markers have been observed previously.^{6,55} Decreased patient

survival has been attributed to the upregulation of these stemness markers in vivo. Here, we have successfully demonstrated that the stromal cell type as well as the drug type can influence the stemness marker expression of GBM cells and these aspects must be considered while evaluating therapies for GBM.

Overall, such a heterogenous MCTS model can be utilized to investigate the impact of cellular cues on the drug response of GBM cells. However, we note the following limitations of our study: (a) An established GBM cell line U87-MG was used in this study which has been commonly used in MCTS models. 56-60 However, the histopathological and biologic profile of these cells have been reported to be different from the original tumor due to prolonged passaging, immortalization, and culture conditions. 61,62 Future studies should consider the implementation of patient-derived GBM cells. (b) Murine astrocytes were used in this study allowing us to determine that the changes in expression of stemness markers were solely through GBM cells cultured in presence of astrocytes as a response to the drug treatments. However, future studies should consider the incorporation of human astrocytes. (c) HUVECs were utilized in this study and future studies should consider the incorporation of primary brain ECs. Incorporating such physiological relevant cell types in combination with patient-derived GBM cells would help develop platforms for therapeutic testing in the future. (d) Based on prior work, ²⁵ we have tested only one concentration of LNF or TMZ, but future studies might consider testing different concentrations as well as different combinations of drugs using 3D MCTS models. (e) As the diameter of our co- and tri-culture MCTS is >500 um. hypoxia might be involved in influencing the stemness marker expression and further examination is needed.

5 | CONCLUSIONS

We have evaluated the impact of LNF and TMZ on the stemness marker expression of GBM cells in 3D co- and tri-culture MCTS models, for the first time. In future, this model may be utilized to incorporate additional cell types in the tumor microenvironment and study the effect of stromal cell-induced stemness marker expression changes as a response to chemotherapeutic drugs. Also, such a model can be adapted to incorporate patient-derived tumor cells and stromal cells for patient-specific drug testing and as a platform for personalized medicine. In addition, this model can further our understanding of crosstalk between different cell types, eventually leading to the development of new therapeutic strategies.

AUTHOR CONTRIBUTIONS

Pinaki S. Nakod: Conceptualization (equal); data curation (lead); formal analysis (lead); investigation (lead); methodology (equal); validation (lead); visualization (lead); writing – original draft (lead); writing – review and editing (equal). **Raghu Vamsi Kondapaneni:** Data curation (supporting); formal analysis (supporting); investigation (supporting); methodology (supporting); validation (supporting). **Brandon Edney:** Conceptualization (supporting); methodology (supporting); writing – review and editing

(supporting). Yonghyun Kim: Funding acquisition (equal); methodology (supporting); resources (supporting); writing – review and editing (equal). Shreyas S. Rao: Conceptualization (equal); funding acquisition (equal); methodology (equal); project administration (lead); resources (lead); supervision (lead); validation (equal); writing – review and editing (equal).

ACKNOWLEDGMENTS

This work was supported by the National Science Foundation (CBET 1604677 to Yonghyun Kim and Shreyas S. Rao) and the Alabama EPS-CoR Graduate Research Fellowship (Pinaki S. Nakod). The authors thank Dr. Yuping Bao (University of Alabama) for generously providing the C8D1A astrocytes and Dr. Matthew Jenny (University of Alabama) for the use of his Nanodrop 2000C spectrophotometer.

CONFLICT OF INTEREST

The authors declare no conflict of interest.

DATA AVAILABILITY STATEMENT

The data that support the findings of this study are available from the corresponding author upon reasonable request.

ORCID

Yonghyun Kim https://orcid.org/0000-0001-6344-1258 Shreyas S. Rao https://orcid.org/0000-0001-7649-0171

REFERENCES

- Nakod PS, Kim Y, Rao SS. Three-dimensional biomimetic hyaluronic acid hydrogels to investigate glioblastoma stem cell behaviors. *Biotechnol Bioeng*. 2020;117(2):511-522. doi:10.1002/bit.27219
- Nakod PS, Kim Y, Rao SS. Biomimetic models to examine microenvironmental regulation of glioblastoma stem cells. *Cancer Lett.* 2018; 429:41-53. doi:10.1016/j.canlet.2018.05.007
- Stankovic T, Randelovic T, Dragoj M, et al. In vitro biomimetic models for glioblastoma-a promising tool for drug response studies. *Drug Resist Updat*. 2021;55:100753. doi:10.1016/j.drup.2021.100753
- Wen PY, Weller M, Lee EQ, et al. Glioblastoma in adults: a Society for Neuro-Oncology (SNO) and European Society of Neuro-Oncology (EANO) consensus review on current management and future directions. Neuro Oncol. 2020;22(8):1073-1113. doi:10.1093/neuonc/noaa106
- Rape A, Ananthanarayanan B, Kumar S. Engineering strategies to mimic the glioblastoma microenvironment. Adv Drug Deliv Rev. 2014; 79-80:172-183. doi:10.1016/j.addr.2014.08.012
- Nakod PS, Kim Y, Rao SS. The impact of astrocytes and endothelial cells on glioblastoma stemness marker expression in multicellular spheroids. *Cell Mol Bioeng*. 2021;14:639-651. doi:10.1007/s12195-021-00691-y
- Ngo MT, Harley BAC. Perivascular signals alter global gene expression profile of glioblastoma and response to temozolomide in a gelatin hydrogel. *Biomaterials*. 2019;198:122-134. doi:10.1016/j. biomaterials.2018.06.013
- Dirkse A, Golebiewska A, Buder T, et al. Stem cell-associated heterogeneity in glioblastoma results from intrinsic tumor plasticity shaped by the microenvironment. *Nat Commun*. 2019;10(1):1787. doi:10.1038/s41467-019-09853-z
- Zhao W, Li Y, Zhang X. Stemness-related markers in cancer. Cancer Transl Med. 2017;3(3):87-95. doi:10.4103/ctm.ctm_69_16

- Matias D, Balca-Silva J, da Graca GC, et al. Microglia/astrocytesglioblastoma crosstalk: crucial molecular mechanisms and microenvironmental factors. Front Cell Neurosci. 2018;12:235. doi:10.3389/ fncel 2018 00235
- Pustchi SE, Avci NG, Akay YM, Akay M. Astrocytes decreased the sensitivity of glioblastoma cells to temozolomide and bay 11–7082. Int J Mol Sci. 2020;21(19):7154. doi:10.3390/ijms21197154
- Yang N, Yan T, Zhu H, et al. A co-culture model with brain tumorspecific bioluminescence demonstrates astrocyte-induced drug resistance in glioblastoma. J Transl Med. 2014;12:278. doi:10.1186/ s12967-014-0278-v
- Civita P, Leite DM, Pilkington GJ. Pre-clinical drug testing in 2D and 3D human in vitro models of glioblastoma incorporating nonneoplastic astrocytes: tunneling Nano tubules and mitochondrial transfer modulates cell behavior and therapeutic respons. *Int J Mol* Sci. 2019;20(23):6017. doi:10.3390/ijms20236017
- Lee DW, Lee SY, Doh I, Ryu GH, Nam DH. High-dose compound heat map for 3D-cultured glioblastoma multiforme cells in a micropillar and microwell chip platform. *Biomed Res Int*. 2017;2017:7218707. doi:10.1155/2017/7218707
- Borovski T, Beke P, van Tellingen O, et al. Therapy-resistant tumor microvascular endothelial cells contribute to treatment failure in glioblastoma multiforme. *Oncogene*. 2013;32(12):1539-1548. doi:10. 1038/onc.2012.172
- Shi Y, Wu M, Liu Y, et al. ITGA5 predicts dual-drug resistance to temozolomide and bevacizumab in glioma. Front Oncol. 2021;11: 769592. doi:10.3389/fonc.2021.769592
- Towner RA, Smith N, Saunders D, et al. OKN-007 increases temozolomide (TMZ) sensitivity and suppresses TMZ-resistant glioblastoma (GBM) tumor growth. *Transl Oncol.* 2019;12(2):320-335. doi:10.1016/j.tranon.2018.10.002
- Sharma A, Shiras A. Cancer stem cell-vascular endothelial cell interactions in glioblastoma. *Biochem Biophys Res Commun.* 2016;473(3): 688-692. doi:10.1016/j.bbrc.2015.12.022
- Zhang X, Ding K, Wang J, Li X, Zhao P. Chemoresistance caused by the microenvironment of glioblastoma and the corresponding solutions. *Biomed Pharmacother*. 2019;109:39-46. doi:10.1016/j.biopha. 2018.10.063
- Lazzari G, Nicolas V, Matsusaki M, Akashi M, Couvreur P, Mura S. Multicellular spheroid based on a triple co-culture: a novel 3D model to mimic pancreatic tumor complexity. *Acta Biomater*. 2018;78:296-307. doi:10.1016/j.actbio.2018.08.008
- Avci NG, Fan Y, Dragomir A, Akay YM, Akay M. Investigating the influence of HUVECs in the formation of glioblastoma spheroids in high-throughput three-dimensional microwells. *IEEE Trans Nanobiosci*. 2015;14(7):790-796. doi:10.1109/TNB.2015.2477818
- Sivakumar H, Devarasetty M, Kram DE, Strowd RE, Skardal A. Multicell type glioblastoma tumor spheroids for evaluating sub-populationspecific drug response. Front Bioeng Biotechnol. 2020;8:538663. doi: 10.3389/fbioe.2020.538663
- Singh N, Miner A, Hennis L, Mittal S. Mechanisms of temozolomide resistance in glioblastoma - a comprehensive review. Cancer Drug Resist. 2021;4:17-43. doi:10.20517/cdr.2020.79
- 24. Gao XY, Zang J, Zheng MH, et al. Temozolomide treatment induces HMGB1 to promote the formation of glioma stem cells via the TLR2/NEAT1/Wnt pathway in glioblastoma. Front Cell Dev Biol. 2021;9:620883. doi:10.3389/fcell.2021.620883
- Chaponis D, Barnes JW, Dellagatta JL, et al. Lonafarnib (SCH66336) improves the activity of temozolomide and radiation for orthotopic malignant gliomas. J Neurooncol. 2011;104(1):179-189. doi:10.1007/ s11060-010-0502-4
- Yust-Katz S, Liu D, Yuan Y, et al. Phase 1/1b study of lonafarnib and temozolomide in patients with recurrent or temozolomide refractory glioblastoma. Cancer. 2013;119(15):2747-2753. doi:10.1002/cncr. 28031

- 27. Lee SY. Temozolomide resistance in glioblastoma multiforme. *Genes Dis.* 2016;3(3):198-210. doi:10.1016/j.gendis.2016.04.007
- Kanzawa T, Germano IM, Kondo Y, Ito H, Kyo S, Kondo S. Inhibition of telomerase activity in malignant glioma cells correlates with their sensitivity to temozolomide. *Br J Cancer*. 2003;89(5):922-929. doi:10. 1038/sj.bjc.6601193
- 29. Ujifuku K, Mitsutake N, Takakura S, et al. miR-195, miR-455-3p and miR-10a(*) are implicated in acquired temozolomide resistance in glioblastoma multiforme cells. *Cancer Lett*. 2010;296(2):241-248. doi: 10.1016/j.canlet.2010.04.013
- Qu H, Song X, Song Z, et al. Berberine reduces temozolomide resistance by inducing autophagy via the ERK1/2 signaling pathway in glioblastoma. Cancer Cell Int. 2020;20(1):592. doi:10.1186/s12935-020-01693-y
- Santangelo R, Rizzarelli E, Copani A. Role for Metallothionein-3 in the resistance of human U87 glioblastoma cells to temozolomide. ACS Omega. 2020;5(29):17900-17907. doi:10.1021/ acsomega.9b04483
- David E, Sun SY, Waller EK, Chen J, Khuri FR, Lonial S. The combination of the farnesyl transferase inhibitor lonafarnib and the proteasome inhibitor bortezomib induces synergistic apoptosis in human myeloma cells that is associated with down-regulation of p-AKT. *Blood.* 2005;106(13):4322-4329. doi:10.1182/blood-2005-06-2584
- Marcuzzi A, De Leo L, Decorti G, Crovella S, Tommasini A, Pontillo A. The farnesyltransferase inhibitors tipifarnib and lonafarnib inhibit cytokines secretion in a cellular model of mevalonate kinase deficiency. *Pediatr Res.* 2011;70(1):78-82. doi:10.1203/PDR. 0b013e31821b581c
- Vlachostergios PJ, Papandreou CN. Efficacy of low dose temozolomide in combination with bortezomib in U87 glioma cells: a flow cytometric analysis. Arch Med Sci. 2015;11(2):307-310. doi:10.5114/ aoms.2013.36919
- Bradshaw A, Wickremesekera A, Brasch HD, et al. Cancer stem cells in glioblastoma multiforme. Front Surg. 2016;3:48. doi:10.3389/fsurg. 2016.00048
- Hemmati HD, Nakano I, Lazareff JA, et al. Cancerous stem cells can arise from pediatric brain tumors. *Proc Natl Acad Sci USA*. 2003; 100(25):15178-15183. doi:10.1073/pnas.2036535100
- Tunici P, Bissola L, Lualdi E, et al. Genetic alterations and in vivo tumorigenicity of neurospheres derived from an adult glioblastoma. *Mol Cancer*. 2004;3:25. doi:10.1186/1476-4598-3-25
- 38. Mehta G, Hsiao AY, Ingram M, Luker GD, Takayama S. Opportunities and challenges for use of tumor spheroids as models to test drug delivery and efficacy. *J Control Release*. 2012;164(2):192-204. doi:10. 1016/j.jconrel.2012.04.045
- Kyffin JA, Cox CR, Leedale J, et al. Preparation of primary rat hepatocyte spheroids utilizing the liquid-overlay technique. *Curr Protoc Toxicol*. 2019;81(1):e87. doi:10.1002/cptx.87
- Lee J, Kotliarova S, Kotliarov Y, et al. Tumor stem cells derived from glioblastomas cultured in bFGF and EGF more closely mirror the phenotype and genotype of primary tumors than do serum-cultured cell lines. *Cancer Cell.* 2006;9(5):391-403. doi:10. 1016/j.ccr.2006.03.030
- Bhuvanalakshmi G, Arfuso F, Millward M, Dharmarajan A, Warrier S. Secreted frizzled-related protein 4 inhibits glioma stem-like cells by reversing epithelial to mesenchymal transition, inducing apoptosis and decreasing cancer stem cell properties. *PLoS One.* 2015;10(6): e0127517. doi:10.1371/journal.pone.0127517
- 42. Hong X, Chedid K, Kalkanis SN. Glioblastoma cell line-derived spheres in serumcontaining medium versus serum-free medium: a comparison of cancer stem cell properties. *Int J Oncol.* 2012;41(5):1693-1700. doi:10.3892/ijo.2012.1592

- Yilmazer A. Evaluation of cancer stemness in breast cancer and glioblastoma spheroids in vitro. 3 Biotech. 2018;8(9):390. doi:10.1007/ s13205-018-1412-v
- Akay M, Hite J, Avci NG, et al. Drug screening of human GBM spheroids in brain cancer chip. Sci Rep. 2018;8(1):15423. doi:10.1038/s41598-018-33641-2
- Narayan RS, Fedrigo CA, Brands E, et al. The allosteric AKT inhibitor MK2206 shows a synergistic interaction with chemotherapy and radiotherapy in glioblastoma spheroid cultures. BMC Cancer. 2017; 17(1):204. doi:10.1186/s12885-017-3193-9
- Shaw P, Kumar N, Privat-Maldonado A, Smits E, Bogaerts A. Cold atmospheric plasma increases temozolomide sensitivity of threedimensional glioblastoma spheroids via oxidative stress-mediated DNA damage. Cancers (Basel). 2021;13(8):1780. doi:10.3390/ cancers13081780
- Azizipour N, Avazpour R, Weber MH, Sawan M, Ajji A, Rosenzweig DH. Uniform tumor spheroids on surface-optimized microfluidic biochips for reproducible drug screening and personalized medicine. *Micromachines (Basel)*. 2022;13(4):587. doi:10.3390/ mi13040587
- Mittler F, Obeid P, Rulina AV, Haguet V, Gidrol X, Balakirev MY. High-content monitoring of drug effects in a 3D spheroid model. Front Oncol. 2017;7:293. doi:10.3389/fonc.2017.00293
- Oh HC, Shim JK, Park J, et al. Combined effects of niclosamide and temozolomide against human glioblastoma tumorspheres. *J Cancer Res Clin Oncol*. 2020;146(11):2817-2828. doi:10.1007/s00432-020-03330-7
- Marino A, Camponovo A, Degl'Innocenti A, et al. Multifunctional temozolomide-loaded lipid superparamagnetic nanovectors: dual targeting and disintegration of glioblastoma spheroids by synergic chemotherapy and hyperthermia treatment. *Nanoscale*. 2019;11(44): 21227-21248. doi:10.1039/c9nr07976a
- Auffinger B, Tobias AL, Han Y, et al. Conversion of differentiated cancer cells into cancer stem-like cells in a glioblastoma model after primary chemotherapy. *Cell Death Differ*. 2014;21(7):1119-1131. doi:10.1038/cdd.2014.31
- Baisiwala S, Auffinger B, Caragher SP, et al. Chemotherapeutic stress induces transdifferentiation of glioblastoma cells to endothelial cells and promotes vascular mimicry. Stem Cells Int. 2019;2019:6107456-6107414. doi:10.1155/2019/6107456
- Ulasov IV, Mijanovic O, Savchuk S, et al. TMZ regulates GBM stemness via MMP14-DLL4-Notch3 pathway. Int J Cancer. 2020;146(8): 2218-2228. doi:10.1002/ijc.32636
- Ma Y, Cheng Z, Liu J, et al. Inhibition of farnesyltransferase potentiates NOTCH-targeted therapy against glioblastoma stem cells. Stem Cell Rep. 2017;9(6):1948-1960. doi:10.1016/j.stemcr. 2017.10.028
- Angelucci C, D'Alessio A, Lama G, et al. Cancer stem cells from peritumoral tissue of glioblastoma multiforme: the possible missing link between tumor development and progression. *Oncotarget*. 2018; 9(46):28116-28130. doi:10.18632/oncotarget.25565
- Ayuso JM, Basheer HA, Monge R, et al. Study of the chemotactic response of multicellular spheroids in a microfluidic device.
 PLoS One. 2015;10(10):e0139515. doi:10.1371/journal.pone.
 0139515
- De Silva T, Ye G, Liang YY, Fu G, Xu G, Peng C. Nodal promotes glioblastoma cell growth. Front Endocrinol (Lausanne). 2012;3:59. doi:10. 3389/fendo 2012 00059
- Boutin ME, Voss TC, Titus SA, Cruz-Gutierrez K, Michael S, Ferrer M. A high-throughput imaging and nuclear segmentation analysis protocol for cleared 3D culture models. *Sci Rep.* 2018;8(1):11135. doi:10.1038/s41598-018-29169-0
- Cisneros Castillo LR, Oancea AD, Stullein C, Regnier-Vigouroux A. A novel computer-assisted approach to evaluate multicellular tumor

- spheroid invasion assay. *Sci Rep.* 2016;6:35099. doi:10.1038/srep35099
- Cheng V, Esteves F, Chakrabarty A, Cockle J, Short S, Bruning-Richardson A. High-content analysis of tumour cell invasion in three-dimensional spheroid assays. *Onco Targets Ther.* 2015;2(6):596-606. doi:10.18632/oncoscience.171
- 61. Allen M, Bjerke M, Edlund H, Nelander S, Westermark B. Origin of the U87MG glioma cell line: good news and bad news. *Sci Transl Med*. 2016;8(354):354re3. doi:10.1126/scitranslmed.aaf6853
- Binder ZA, Wilson KM, Salmasi V, et al. Establishment and biological characterization of a panel of glioblastoma multiforme (GBM) and GBM variant oncosphere cell lines. *PLoS One*. 2016;11(3):e0150271. doi:10.1371/journal.pone.0150271

SUPPORTING INFORMATION

Additional supporting information can be found online in the Supporting Information section at the end of this article.

How to cite this article: Nakod PS, Kondapaneni RV, Edney B, Kim Y, Rao SS. The impact of temozolomide and lonafarnib on the stemness marker expression of glioblastoma cells in multicellular spheroids. *Biotechnol. Prog.* 2022;e3284. doi:10. 1002/btpr.3284